An Efficient One-Pot Synthesis of Octahydroquinazolinone Derivatives Using Magnetic Cobalt Ferrite as Catalyst

U.M. Mandle[1], S.B. Rathod[2], N.S. Kolate[2], P.A. Nanaware[2], V.S. Rane[2],
P.A. Amble[2], K.S. Lohar[3] and B.L. Shinde[2,*]

[1]Department of Chemistry, Sangmeshwar College, Solapur-413001, India
[2]Department of Chemistry, Waghire College of Arts, Commerce and Science, Saswad, Pune-412301, India
[3]Department of Chemistry, Shrikrishna Mahavidyalaya, Gunjoti, Osmanabad-413606, India

*Corresponding author: E-mail: shindebl1981@gmail.com

In this work, octahydroquinazolinone derivatives were synthesized using magnetic cobalt ferrite nanoparticles using oxalate precursor method. The XRD pattern and IR spectrum confirmed the formation of single segment cubic spinel cobalt ferrite. The average size of the crystallites was determined to be 26.599 nm, while the lattice constant was found to be 8.365 Å. A fine spherical $CoFe_2O_4$ particles with some quantity of aggregation may be observed within the SEM and TEM images. Nano spinel cobalt ferrite nanoparticles is a easily synthesized, non-toxic, less expensive, effortlessly magnetically recoverable and green catalyst for the synthesis of octahydroquinazolinone derivatives through the condensation of aromatic aldehydes with urea or thiourea and dimedone. The advantages of this technique are quick reaction time, ease of product isolation and high yields.

Keywords: Octahydroquinazolinone, Cobalt ferrite, Magnetic, Aromatic aldehyde.

INTRODUCTION

Multicomponent reactions (MCRs) refer to a class of reactions in which three or more reactants are combined in a single reaction vessel, enabling the synthesis of a desired product in a single step [1]. The one of the most essential operations in organic chemistry is formation of a new carbon-carbon bond. As an end result, there is a little or unsolicited byproduct do form related to sequential synthesis. Metal-catalyzed reactions (MCRs) have garnered a significant interest in the field of organic synthesis due to their advantageous atom economy, operational simplicity and overall remarkable productivity [2,3]. The conventional way to prepare the complex molecules through sequential preparation, where MCRs let the assembly of complex molecules in a one-pot mode. On the other hand, individual bonds inside the target molecule formed in the standard stepwise mode through a multi-step synthetic method. The significant feature of MCRs is the ability to generate certain bonds in a single step, without the groing through the intermediate reactions, alteration of reaction conditions or the introduction of the additional reagents. Sustainable techniques are considered excellent tools for the synthesis of biological-active compounds and the optimization of strategies within the pharmaceutical industry [4,5].

Multicomponent reactions (MCRs) are considered to be a significant tool in the field of sustainable organic synthesis. By employing MCRs along with green chemistry principles, organic chemists might potentially bring themselves closer to achieving the ideal synthesis [6]. Several multicomponent organic reactions involve different types of catalysts that possess many active sites, nano-scale dimensions and a substantial surface area [7].

Spinel ferrite nanoparticles have gained attention due to their better magnetic, electronic and catalytic characteristics compared to their bulk form. The catalytic efficiency of ferrites for many reactions is related to the alteration of oxidation of iron among 2+ and 3+. Additional vital quality of ferrite materials from industrial point-of-view is their balance underneath particularly lowering situations because of their spinel crystallography. In evaluation to the spinel ferrites, catalyst Fe_2O_3

loses its nature as it is altered to FeO and metal iron. Nanoparticles of magnetite Fe_2O_3 as a catalyst can be simply bifurcated using outside magnet without the need of filtration [8]. Cobalt ferrite, $CoFe_2O_4$, amongst the spinel ferrites forms inverse spinel structure where majority of Co^{2+} ions are located at B site, whereas Fe^{3+} ions are equally disbursed among A and B sites [9].

Octahydroquinazolinone derivatives known for the pinnacle medicinal agents, which can be used for antimicrobial [10], anti-inflammatory analgesic [11], antiviral [12], *etc*. Synthesis of octahydroquinazolinone derivatives by MCRs has gained reputation because of its easy process, economic efficiency and better selectivity [12]. Bigenelli reactions preferentially applicable for β-diketone relatively than open-chain dicarbonyl complexes for the synthesis octahydroquinazolinone [13]. The synthesis of octahydroquinazolinone through one-pot three-component reaction of aldehydes, dimedone and urea or thiourea by the usage of special catalysts or chemical agents like conc. HCl [13], conc. H_2SO_4 [14], trimethylsilyl chloride (TMCl) [15] and Lewis acids (La(OTf)$_3$, La$_2$O$_3$, ZrCl$_4$) [16,17] are already reported. However, many of these techniques have been associated by one or more drawbacks, such as the requirement for harsh reaction conditions, prolonged reaction times, low yields, the use of hazardous and expensive catalysts, excessively acidic environments and the formation of several byproducts. So the improvement of easy, high-yielding and environmentally friendly techniques remains ideal and much in demand.

Keeping the importance of octahydroquinazolinone derivatives, it was decided to synthesize octahydroquinazolinone derivatives (**4a-n**) by one-pot three-component reaction of dimedone, aromatic aldehyde and urea/thiourea using magnetically recoverable and reusable spinel cobalt ferrite catalyst prepared by oxalate precursor technique.

EXPERIMENTAL

Preparation of CoFe$_2$O$_4$ ferrite catalyst: Nanospinel cobalt ferrite was synthesized by the oxalate precursor method [18]. Stoichiometric amount of corresponding cobalt sulphate and ferrous sulphate dissolved in deionized water at 60 ºC to obtain clear solution. Saturated oxalic acid solution added with continuous string till all metal sulphates converted in to metal oxalates, then the precipitate digested for 0.5 h, washed with deionized water till free from sulphates (tested with barium chloride). The oxalate precursor precipitate filtered, dried at room temperature and finally calcinated at 600 ºC for 4 h, to obtain spinel cobalt ferrites.

Characterization: The structural parameters of calcinated cobalt ferrite investigated by X-ray diffraction Phillips-3710 X-ray diffractometer employed with Cu$K\alpha$ radiation (λ = 1.5405 Å) were used in the present study. Microstructure investigated by JEOL-JSM-5600-N Scanning Electron Microscope. The infrared spectra recorded at room temperature by Perkin-Elmer infrared spectrophotometer in the range of 4000-400 cm^{-1}. Magnetic measurements carried at room temperature using the vibrating sample magnetometer. ^{1}H NMR spectra of representative derivatives were recorded on Bruker-Avance III HD NMR 500 MHz spectrometer.
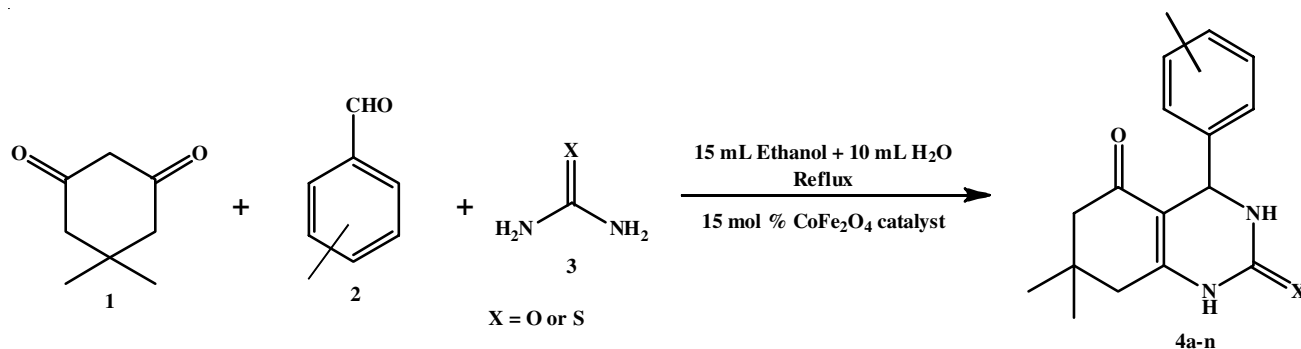
Synthesis of octahydroquinazolinone derivatives: A mixture of dimedone (**1**) (10 mmol), aromatic aldehydes (**2**) (10 mmol) and urea/thiourea (**3**) (15 mmol) dissolved in solvent (15 mL ethanol + 10 mL distilled water) in round bottom flask followed by the addition of prepared cobalt ferrite catalysts (CoFe$_2$O$_4$, 15 mol%)and the reaction mixture was then heated underneath reflux. The reaction monitored by the TLC, [solvent system ethyl acetate:*n*-hexane (3:7)] (**Scheme-I**).

The catalyst was removed by firmly attaching it to the bottom of the flask using a strong magnet. Subsequently, the reaction mixture was extracted and allowed to cool down to the ambient temperature and finally filtered. The residue of octahydroquinazolinone derivatives **4a-n** was then washed thoroughly with aqueous ethanol and dried. The product obtained first purified by using recrystallization followed by column chromatography.

4-Phenyl-7,7-dimethyl-4,6,7,8-tetrahydro-1*H*,3*H*-quinazolin-2,5-dione (4a): m.p. 290 ºC, ^{1}H NMR: (500 MHz, DMSO-d_6) δ ppm: 0.98 (s, 3H, CMe); 1.10 (s, 3H, CMe); 2.22 (q, 2H, CH$_2$); 2.39 (q, 2H, CH$_2$); 5.48 (d,1H, CH); 7.25 (m, 5H, Ar); 7.45 (s, 1H, NH); 10.38 (s, 1H, NH).

4-(4-Dimethylamino-phenyl)-7,7-dimethyl-4,6,7,8-tetrahydro-1*H*,3*H*-quinazolin-2,5-dione (4b): m.p.. 238 ºC, ^{1}H NMR: (500 MHz, DMSO-d_6) δ ppm: 0.98 (s, 3H, CMe); 1.11 (s, 3H, CMe); 2.18 (q, 2H, CH$_2$); 2.36 (q, 2H, CH$_2$); 2.52 (s, 6H, NMe$_2$), 5.32 (d, 1H, CH); 7.36 (m, 4H, Ar); 7.85 (s, 1H, NH); 10.24 (s, 1H, NH).

4-(4-Chloro-phenyl)-7,7-dimethyl-4,6,7,8-tetrahydro-1*H*,3*H*-quinazolin-2,5-dione (4f): m.p. 260 ºC; ^{1}H NMR: (500 MHz, DMSO-d_6) δ ppm: 0.99 (s, 3H, CMe); 1.09 (s, 3H, CMe);

Scheme-I: Synthesis of octahydroquinazolinone derivatives (**4a-n**) from dimedone (**1**), aromatic aldehyde (**2**) and urea/thiourea (**3**) using cobalt ferrite catalyst

1.65 (q, 2H, CH$_2$); 2.3 (q, 2H, CH$_2$); 5.5 (d, 1H, CH); 6.9 (m, 4H, Ar); 7. 4 (s, 1H, NH); 11.5 (s, 1H, NH).

4-(4-Methoxyphenyl)-7,7-dimethyl-4,6,7,8-tetrahydro-1*H*,3*H*-quinazolin-2,5-dione (4g): m.p. 240 ℃; ^{1}H NMR (500 MHz, DMSO-d_6) δ ppm: 0.97 (s, 3H, CMe); 1.10 (s, 3H, CMe); 1.18 (q, 2H, CH$_2$); 2.84 (s, 2H, CH$_2$); 3.88 (s, 3H, OCH$_3$), 5.32 (d, 1H, CH); 6.8 (m, 4H, Ar); 9.32 (s, 1H, NH); 11.24 (s, 1H, NH).

4-(4-Nitrophenyl)-7,7-dimethyl-2-thioxo-4,6,7,8-tetra-hydro-1*H*,3*H*-quinazolin-5-one (4l): m.p. 212 ℃; ^{1}H NMR: (500 MHz, DMSO-d_6) δ ppm: 0.99 (s, 3H, CMe); 1.09 (s, 3H, CMe); 2.2 (s, 1H, NH); 2.3 (m, 2H, CH$_2$); 2.3 (m, 2H, CH$_2$); 5.5 (d, 1H, CH); 7.3 (m, 4H, Ar); 8.4 (s, 1H, NH); 11.8 (d, 1H, NH).

4-(4-Methoxyphenyl)-7,7-dimethyl-2-thioxo-4,6,7,8-tetrahydro-1*H*,3*H*-quinazolin-5-one (4n): m.p. 282 ℃; ^{1}H NMR (500 MHz, DMSO-d_6) δ ppm: 0.98 (s, 3H, CMe); 1.12 (s, 3H, CMe); 2.24(q, 2H, CH$_2$); 3.14 (s, 2H, CH$_2$); 3.85 (s, 3H, OCH$_3$), 5.22 (d, 1H, CH); 6.12 (m, 4H, Ar); 9.42 (s, 1H, NH); 11.14 (s, 1H, NH).

RESULTS AND DISCUSSION

FTIR and thermal analysis of oxalate precursor: The FTIR spectrum of synsesized oxalate precursor [CoFe$_2$(C$_2$O$_4$)$_3$·2H$_2$O] was analyzed in the range of 4000-400 cm^{-1} (Fig. 1). The two peaks at 3404 cm^{-1} and 3343 cm^{-1} assigned to OH$_2$ symmetric stretch and OH$_2$ asymmetric stretching, respectively. The strong single peak at 1640 cm^{-1} is related to the >C=O stretching vibration. The two proximate peaks at 1373 and 1320 cm^{-1} are related to the C–O symmetric and asymmetric vibrations, respectively. The peak at 821 cm^{-1} is due to the O–C–O vibration. Another two IR peaks at 494 and 532 cm^{-1} are from the Fe–O stretching and Co–O stretching, respectively.

Fig. 2. TGA/DTA plot of oxalate precursor [CoFe$_2$(C$_2$O$_4$)$_3$·2H$_2$O]

step obtained at around 95.32 and 185.46 ℃, due to the dehydration of oxalates precursor. The second step decomposition, in which anhydrous oxalate can be converted into metal oxide and gases (CO$_2$ and CO) from 243.56 to 471.76 ℃, which finally results into formation of cobalt ferrite nanoparticles.

Structural analysis of CoFeO$_4$ spinel ferrite catalyst: FTIR of calcinated cobalt ferrite was obtained in the range of 800-400 cm^{-1} at room temperature (Fig. 3). Two foremost IR absorption bands determined, band ν_1 at 591 cm^{-1} is allocated to the tetrahedral A-site, even as the decrease wave range ν_2 at 425 cm^{-1} is allocated to the octahedral B-site. Within the cobalt ferrite pattern, the excessive wave quantity ν_1 signifies the vibration of Fe^{3+}–O^{2-} inside the sub-lattice site A, whilst the band ν_2 signifies the Fe^{3+}/Co^{3+} metal–oxygen vibrations at the B-sites. The change in ν_1 and ν_2 band locations is anticipated due to the change within the Fe^{3+}–O^{2-} distances for the A- and B-sites [19].

Fig. 1. IR spectrum of oxalate precursor [CoFe$_2$(C$_2$O$_4$)$_3$·2H$_2$O]

Fig. 3. IR spectrum of CoFe$_2$O$_4$ catalyst

Fig. 2 represents the thermal profiles (TGA/DTA) of oxalates precursor. It is observed that the oxalate precursor decomposed thermally in several steps. First decomposition
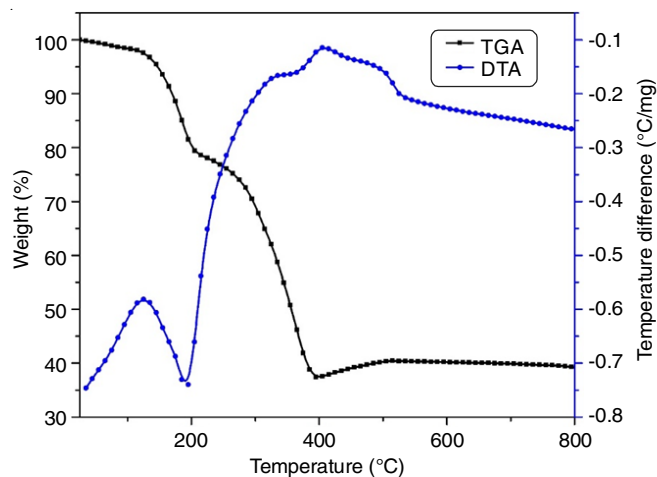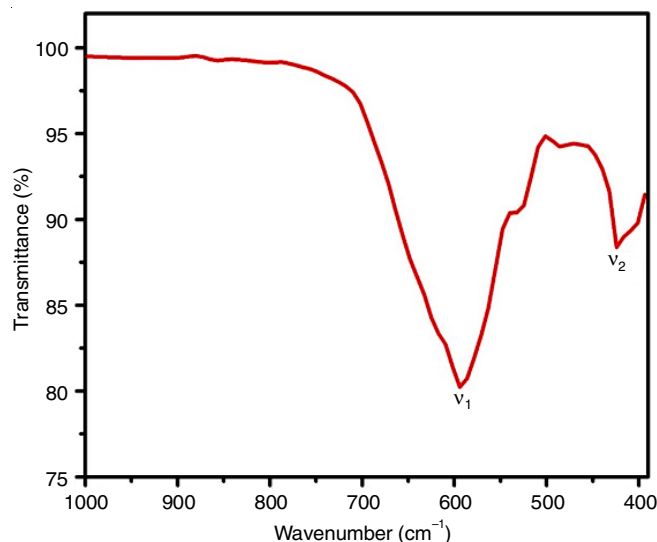
The XRD pattern of the calcinated cobalt ferrite sample at 600 ℃ is presented in Fig. 4. All the XRD peaks are characteristic of cubic spinel CoFe$_2$O$_4$ (JCPDS card#79-1744) and no secondary peaks related to impurity phases observed in the
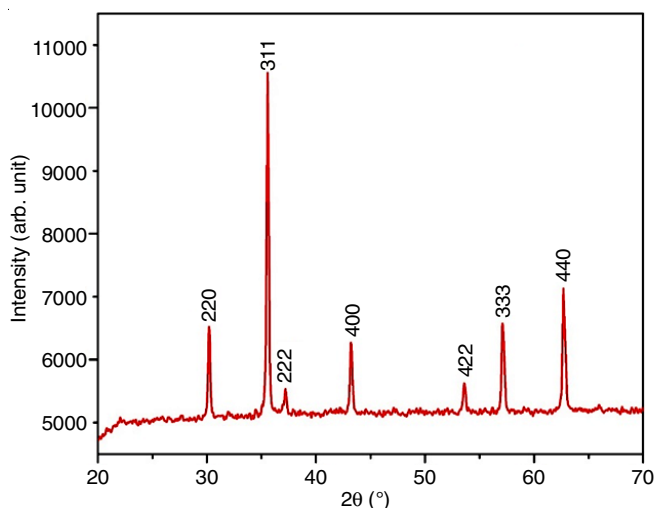
Fig. 4. XRD patterns of calcinated CoFe$_2$O$_4$ catalyst

XRD patterns [19]. The observed XRD diffraction peaks were assigned to (220), (311), (222), (400), (422), (333) and (400) planes of cobalt spinel ferrite. The average crystallite size from the most intense (3 1 1) peak were calculated using XRD data and Debye-Scherrer formula [20], which is found to 26.599 nm.

The Lattice parameter 'a' was calculated by using XRD data the equation discussed elsewhere [20], $a = d\sqrt{N}$, where, 'a' is lattice parameter, 'd' is the inter planer spacing and $\sqrt{N} = \sqrt{(h^2 + k^2 + l^2)}$. The calculated value of lattice parameter of cobalt ferrite is A = 8.365 Å, shows that the sample is to be cubic spinel structure.

As it can be observed from the SEM and TEM micrographs (Fig. 5), calcinated CoFe$_2$O$_4$ nanoparticles synthesized by the oxalate precursor technique show a uniform structure with fine particle size distribution. Agglomerated spherical CoFe$_2$O$_4$ particles were also seen in the SEM and TEM images.

The magnetic properties of calcinated spinal cobalt ferrite particles were assessed at room temperature using a vibrating sample magnetometer (VSM). Hysteresis loop of calcinated cobalt ferrite is shown in Fig. 6. The saturation magnetization (M$_s$) at room temperature was found to be 55.83 emu/g and remanent magnetization (M$_r$) become 17.95 emu/g and co-ercivity (H$_c$) turned into 695.92 O$_e$. The saturation magnetization (M$_s$) value of CoFe$_2$O$_4$ nanoparticles was found to be 55.83 emu/g, which is comparatively lower than the reported value for the bulk samples (80 emu/g). This discrepancy might be attributed to the superparamagnetic characteristics shown by the magnetic nanoparticles.
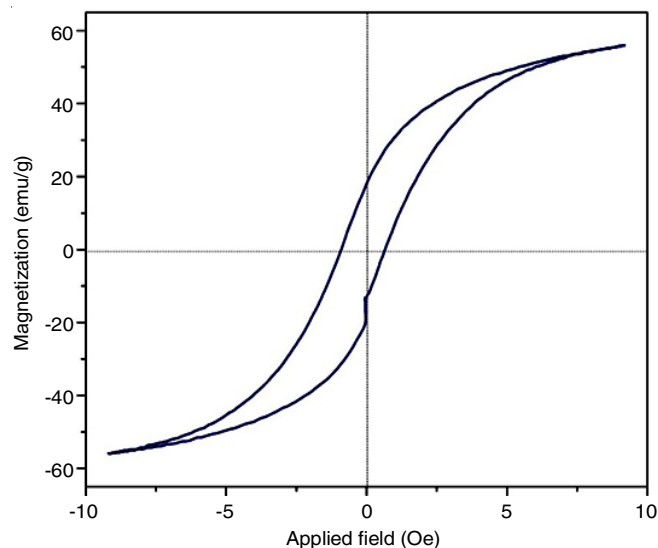
Fig. 6. Hysteresis loop of calcinated CoFe$_2$O$_4$ catalyst

Optimum conditions for the synthesis of octahydro-quinazolinone derivatives: To begin with the quantity of cobalt ferrite (catalyst load) became optimized for model reaction for compound **4a**, the use of benzaldehyde and urea. The catalyst was introduced in different quantities of 0, 5, 10, 15, and 20 mol%. The results suggest that there is a positive correlation between the concentration of catalyst, ranging from 0 mol% to 15 mol%, and the yield of the process. In the absence of catalyst (0 mol%) in model reaction **4a**, the highest yield of 27% was obtained after a reaction time of 290 min (Table-1).
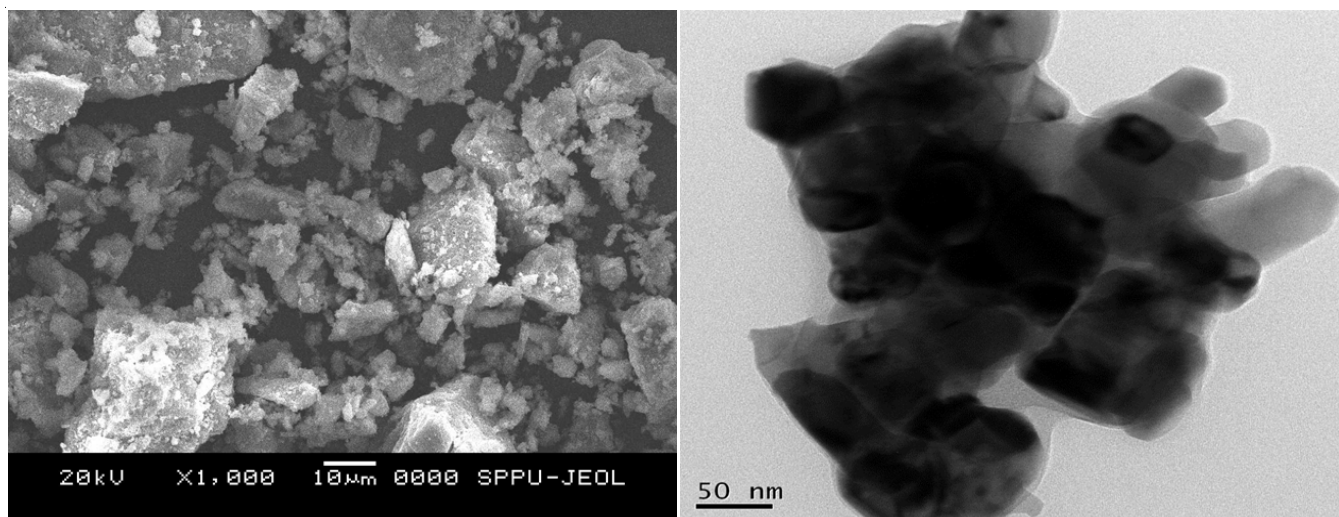

Fig. 5. SEM and TEM micrographs of calcinated CoFe$_2$O$_4$ catalyst

TABLE-1
OPTIMIZATION OF REACTION CONDITIONS AND CATALYST
LOAD (mol%) OF CoFe$_2$O$_4$ NANOPARTICLES FOR THE
SYNTHESIS OF OCTAHYDROQUINAZOLINONE (4a)

Entry	Catalyst loading (mol%)	Time (min)	Yield[a] (%)
1	0	215	27:00
2	05	55	89.65
3	10	50	95.45
4	15	40	98.02
5	20	45	93.50

[a]Hereinafter, isolated yield of pure product.

To evaluate the generality of this method, five different aromatic aldehydes with urea/thiourea have been used under the optimized conditions to acquire substituted octahydroquinazolinones (4a-n) (Scheme-I). As tabulated in Table-2, the reaction of aromatic aldehydes having electron-withdrawing substituents reacted thoroughly at faster rate compared with aromatics aldehydes substituted with electron releasing groups to offer octahydroquinazolinone.
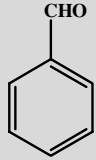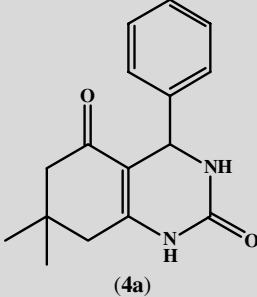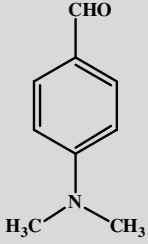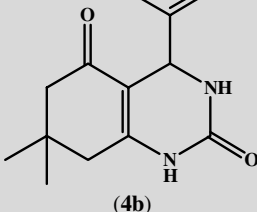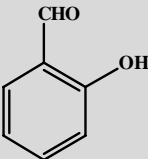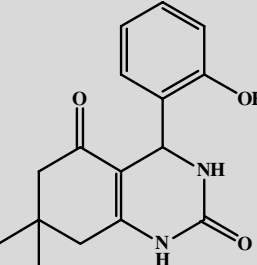
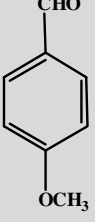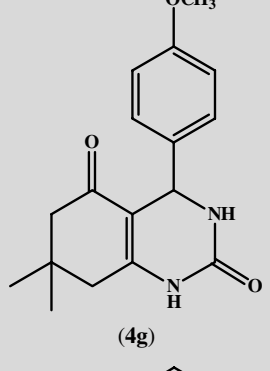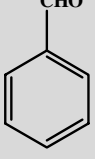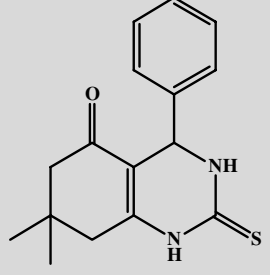**Reusability studies:** Catalyst reusability is of fundamental difficulty in heterogeneous catalysis. The restoration and reusability of the catalyst changed into investigated on this reaction for model reaction (4a). The catalyst was eliminated by setting the catalyst magnetically at the bottom of the flask with a magnet and then the reaction mixture collected and cooled to room temperature. The eliminated catalyst washed thoroughly with acetone and can be recycled for another run. The catalyst can be used for five consecutive times without any considerable lack of its catalytic performance (Cycle number and yield of 4a: 1- 98.02%; 2- 97.56%; 3- 95.60%; 4- 94.20%; 5- 94.75%). Since the catalyst possesses the magnetic properties, enabling them to be easily and effectively separated using an external magnet at room temperature. This characteristic provides a significant advantage for heterogeneous catalysts.
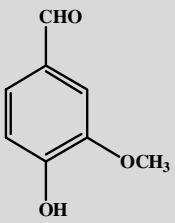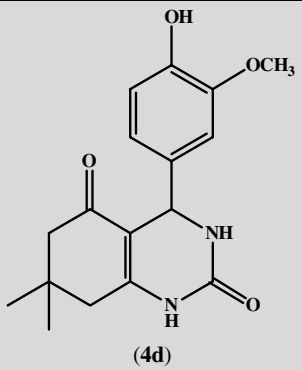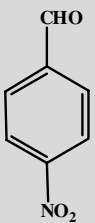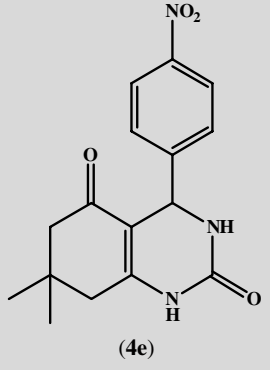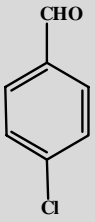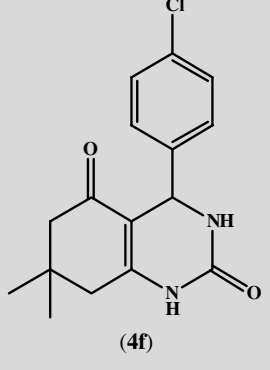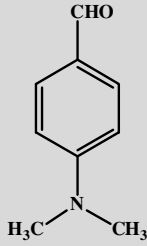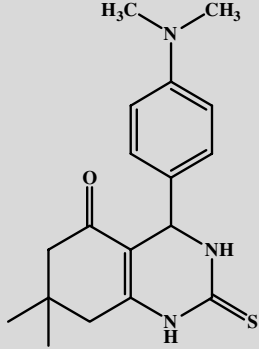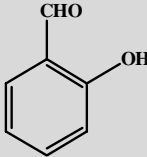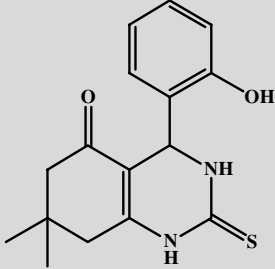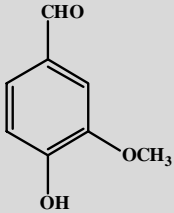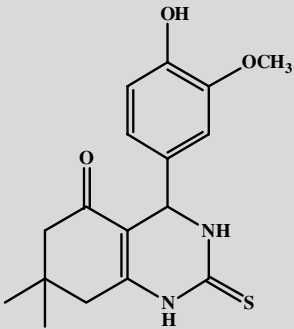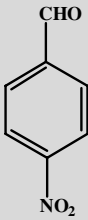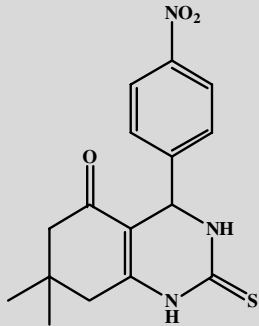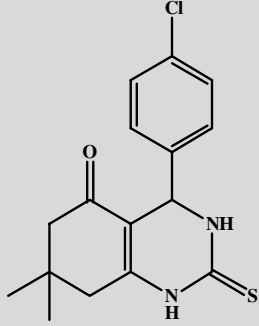
Conclusion
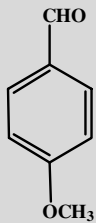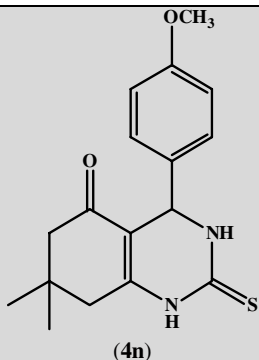
In this work, a non-toxic, low-cost, easily magnetically recoverable and green catalyst spinel cobalt ferrite nanoparticles were efficiently synthesized by oxalate precursor method. The XRD patterns and IR spectrum confirmed the formation of single phase cubic spinel cobalt ferrite. A very fine spherical CoFe$_2$O$_4$ particles with some quantity of aggregation was observed within the SEM and TEM images. Octahydroquinazolinone

TABLE-2
SYNTHESIS OF OCTAHYDROQUINAZOLINONE DERIVATIVES USING CoFe$_2$O$_4$ NANOPARTICLES (4a-n)

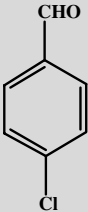| Entry	Aromatic aldehyde	Product	Time (min)	Yield[a] (%)	m.p. (°C)
1		(4a)	40	98.02	290
2		(4b)	50	96.63	238
3		(4c)	45	95.92	256

4	CHO, OCH₃, OH (benzaldehyde)	(4d)	50	97.36	290
5	CHO, NO₂ (benzaldehyde)	(4e)	40	98.32	256
6	CHO, Cl (benzaldehyde)	(4f)	40	97.22	260
7	CHO, OCH₃ (benzaldehyde)	(4g)	50	95.77	240
8	CHO (benzaldehyde)	(4h)	50	97.00	280

9		(4i)	45	98.45	290
10		(4j)	45	97.90	258
11		(4k)	45	98.7	264
12		(4l)	45	98.41	212
13		(4m)	55	96.40	230

| 14 | (4-methoxybenzaldehyde structure) | (4n structure) | 45 | 98.28 | 282 |

ᵃHereinafter, isolated yield of pure product

derivatives (**4a-n**) were efficiently synthesized using CoFe$_2$O$_4$ magnetic nanoparticles as heterogeneous catalyst with good yields and in short time.

CONFLICT OF INTEREST

The authors declare that there is no conflict of interests regarding the publication of this article.

REFERENCES

1. A. Dömling and I. Ugi, *Angew. Chem. Int. Ed.*, **39**, 3168 (2000);
   https://doi.org/10.1002/1521-3773(20000915)39:18<3168::AID-ANIE3168>3.0.CO;2-U
2. M. Poliakoff, J.M. Fitzpatrick, T.R. Farren and P.T. Anastas, *Science*, **297**, 807 (2002);
   https://doi.org/10.1126/science.297.5582.807
3. J.D. Sunderhaus and S.F. Martin, *Chem. Eur. J.*, **15**, 1300 (2009);
   https://doi.org/10.1002/chem.200802140
4. R.C. Cioc, E. Ruijter and R.V. Orru, *Green Chem.*, **16**, 2958 (2014);
   https://doi.org/10.1039/C4GC00013G
5. S.S. van Berkel, B.G. Bögels, M.A. Wijdeven, B. Westermann and F.P. Rutjes, *Eur. J. Org. Chem.*, **2012**, 3543 (2012);
   https://doi.org/10.1002/ejoc.201200030
6. U.M. Mandle, A.M. Pachpinde, D.R. Kulkarni and B.L. Shinde, *Mater. Today Proc.*, **46**, 6122 (2021);
   https://doi.org/10.1016/j.matpr.2020.03.583
7. N. Kerru, L. Gummidi, S.N. Maddila, K.K. Gangu and S.B. Jonnalagadda, *Inorg. Chem. Commun.*, **116**, 107935 (2020);
   https://doi.org/10.1016/j.inoche.2020.107935
8. N. Bahlawane, P.H.T. Ngamou, V. Vannier, T. Kottke, J. Heberle and K. Kohse-Höinghaus, *Phys. Chem. Chem. Phys.*, **11**, 9224 (2009);
   https://doi.org/10.1039/b910707j
9. M. Houshiar, F. Zebhi, Z.J. Razi, A. Alidoust and Z. Askari, *J. Magn. Magn. Mater.*, **371**, 43 (2014);
   https://doi.org/10.1016/j.jmmm.2014.06.059
10. N.C. Desai, A. Dodiya and N. Shihory, *J. Saudi Chem. Soc.*, **17**, 259 (2013);
    https://doi.org/10.1016/j.jscs.2011.04.001
11. S.S. Chine, C.S. Patil and R.P. Pawar, *Eur. Chem. Bull.*, **7**, 318 (2019);
    https://doi.org/10.17628/ecb.2018.7.318-323
12. A. Mobinikhaledi, N. Foroughifar and H. Khodaei, *Eur. J. Chem.*, **1**, 291 (2010);
    https://doi.org/10.5155/eurjchem.1.4.291-293.108
13. P.V. Badadhe, A.V. Chate, D.G. Hingane, P.S. Mahajan, N.M. Chavhan and C.H. Gill, *J. Korean Chem. Soc.*, **55**, 936 (2011);
    https://doi.org/10.5012/jkcs.2011.55.6.936
14. Z. Hassani, M.R. Islami and M. Kalantari, *Bioorg. Med. Chem. Lett.*, **16**, 4479 (2006);
    https://doi.org/10.1016/j.bmcl.2006.06.038
15. I.S. Nosulenko, O.Y. Voskoboynik, G.G. Berest, S.L. Safronyuk, S.I. Kovalenko, O.M. Kamyshnyi and A.V. Katsev, *Sci. Pharm.*, **82**, 483 (2014);
    https://doi.org/10.3797/scipharm.1402-10
16. K. Nikoofar and Z. Khademi, *Res. Chem. Intermed.*, **42**, 3929 (2016);
    https://doi.org/10.1007/s11164-015-2260-6
17. P.M. Shah and M.P. Patel, *Med. Chem. Res.*, **21**, 1188 (2012);
    https://doi.org/10.1007/s00044-011-9628-y
18. S.Y. Srinivasan, K.M. Paknikar, D. Bodas and V. Gajbhiye, *Nanomedicine*, **13**, 1221 (2018);
    https://doi.org/10.2217/nnm-2017-0379
19. G. Allaedini, S.M. Tasirin and P. Aminayi, *Int. Nano Lett.*, **5**, 183 (2015);
    https://doi.org/10.1007/s40089-015-0153-8
20. B.L. Shinde, U.M. Mandle, A.M. Pachpinde and K.S. Lohar, *J. Therm. Anal. Calorim.*, **147**, 2947 (2022);
    https://doi.org/10.1007/s10973-021-10719-0